ACS OMEGA

Open Access

http://pubs.acs.org/journal/acsodf

Article

Research on the Low-Temperature Oxygen Consumption and Low-Oxygen Gas Emission Law in Goaf of Ultrathick Coal Seams

Xu Zheng, Jia Liu,* Peng Liu,* Xiaoping Liu, Ping Luo, Guangzu Hao, Hongwei Liu, and Tingting Cai

Cite This: *ACS Omega* 2024, 9, 33679−33691

Read Online

ACCESS | Metrics & More | Article Recommendations

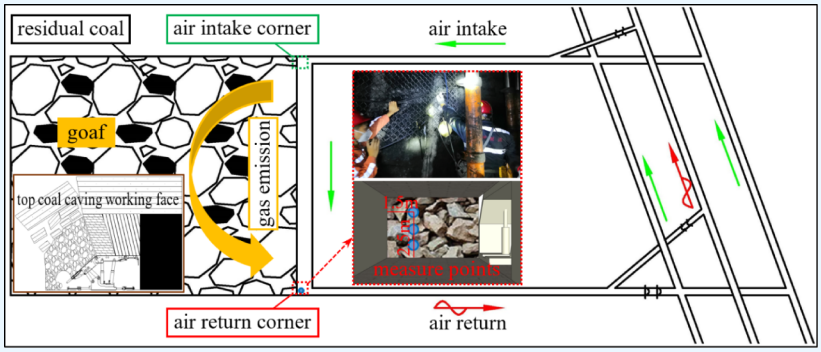

ABSTRACT: Low-oxygen (oxygen concentration below 18.5%) phenomena often occur in the top coal caving working face of ultrathick coal seams, posing a serious threat to the safety of workers. The characteristics of oxygen consumption and gas production at low-constant temperature and the corresponding functional group evolution of residual coal in goaf were studied by temperature-programmed and infrared spectrum experiments. The influence of different factors on the emission of low-oxygen gases was studied through numerical calculation. The results show that low-temperature oxygen consumption and gas production occurred when the coal was about 40 °C. When the temperature was constant, the oxygen consumption and gas production rate increased with the extension of time. In the early stage of coal oxidation, the aliphatic C−H components were attacked by oxygen molecules and reacted with them. The asymmetric methyl and methylene groups were more likely to oxidize and produce carbonyl compounds. With the increase of nitrogen injection, the overall width of the oxidation zone (oxygen concentration was defined as 10−18%) narrowed, and the range of the oxidation zone moved forward from the depth of the goaf. The oxygen concentration in the air return corner decreased gradually, and the low-oxygen area in the air return corner expanded gradually. The distance between the low-oxygen area of the working face and the air intake corner was gradually shortened. With the increase of air intake, the width of the oxidation zone increased and moved to the depth of goaf, and the degree of low oxygen in the air return corner increased. The research results are of great significance for the understanding and prevention of the low-oxygen phenomenon in ultrathick coal seams.

1. INTRODUCTION

China is one of the major coal mining countries in the world. Compared with other countries, China's coal resources are widely distributed, with significant differences in geological conditions and more complex mining conditions.[1] Among them, spontaneous combustion,[2] methane,[3−5] dust,[6] roof,[7] and water disasters[8] are the main challenges faced by China's coal resource extraction. Due to the limitation of mining height, the exploitation of ultrathick coal seams has always been a worldwide problem. With the continuous development of mining technology around the world, fully mechanized top coal caving technology has been widely used in the exploitation of ultrathick coal seams. Although this technology can significantly improve the mining efficiency in ultrathick coal seams, it brings some new problems, such as excessive coal waste, serious air leakage in goaf, and harmful gas emission in the air return corner. In recent years, the outflow of low oxygen and other harmful gases from the air return corner of the top coal caving working face in the ultrathick coal seams has become more and more serious, which has seriously threatened the safety of workers. In general, when the oxygen concentration is below 18.5%, personnel's work ability decreases and breathing begins to be difficult. In addition, in

Received: March 9, 2024
Revised: July 11, 2024
Accepted: July 12, 2024
Published: July 26, 2024

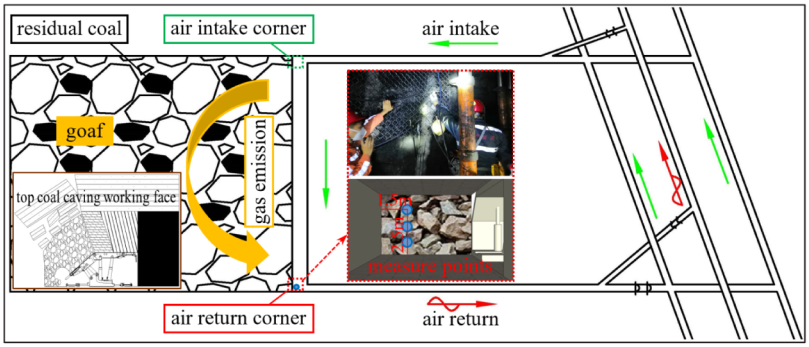

Figure 1. Mining and ventilation system diagram of the 8105 top coal caving working face.

Table 1. O_2 Concentration at Different Locations in the Air Return Corner of the 8105 Working Face

production status	height	O_2/%	N_2/%	CO/%	CH_4/%	CO_2/%	C_2H_6/%
coal cutting	2.5 m	18.43	78.86	0.000524	0.00517	2.71	0.000813
	1.5 m	19.07	78.12	0.000465	0.009281	2.82	-
	0.8 m	17.56	79.33	0.001936	0.008125	2.98	0.001455
top coal caving	2.5 m	16.5	78.59	0.001628	0.00813	4.96	0.000794
	1.5 m	16.13	78.77	0.001231	0.000465	5.17	0.001185
	0.8 m	16.96	79.44	0.00025	0.00193	3.66	0.001576
equipment maintenance	2.5 m	18.54	78.26	0.001165	0.00162	2.85	0.000698
	1.5 m	19.13	78.47	0.001547	0.00123	2.43	-
	0.8 m	19.66	78.14	0.00169	0.001822	2.29	0.000324

order to effectively inhibit the spontaneous combustion of residual coal in the goaf, nitrogen will be injected during the mining process.[9,10] The "technical specifications for nitrogen fire prevention and extinguishing in coal mines" stipulate that the oxygen concentration in the working face during nitrogen injection should not be less than 18.5%. In summary, the phenomenon when the oxygen concentration of the working face is less than 18.5% is defined as a low-oxygen phenomenon.

In order to deal with the low-oxygen phenomenon in the air return corner of the top coal caving working face, a series of studies have been carried out, and it is found that the studies are mainly focused on revealing the cause mechanism. Wang et al.[11] thought that oxygen consumption by spontaneous combustion of a large amount of residual coal was the main cause of the low-oxygen phenomenon. Gulawani et al.[12] found that air leakage in the goaf was the main reason for the accumulation and exceeding of low-oxygen gases in the air return corner of the working face. Wasilewski[13] found that mine air pressure varied synchronously with surface atmospheric pressure and that atmospheric pressure fluctuations were the main power source for low-oxygen gas spillage. Lolon et al.[14] found that the amount of low-oxygen gases emitted from the goaf was controlled by the decreased rate of atmospheric pressure. Lolon et al.[15] pointed out that it was the "breathing" effect of the "expansion−contraction" of the goaf that led to the influx of low-oxygen gases into the working face. Chen et al.[16] thought coal seams located in the CO_2−N_2 zone provided intrinsic low-oxygen gases, nitrogen injection into the goaf provided extrinsic low-oxygen gases, and ventilation and atmospheric pressure changes provided the power for low-oxygen gas emission.

Summarizing and analyzing the current research status, it can be concluded that there is no unified understanding of the mechanism of low-oxygen causation, and spontaneous combustion in goaf is often considered to be the most common causative factor.[11−16] However, in recent years, it has been often found that low oxygen and high carbon monoxide often appear in the air return corner of the working face, but there are no high temperature points and other obvious signs of spontaneous combustion in the goaf. Therefore, the authors propose the following hypothesis: the ultrathick coal seam has already begun to undergo a slow coal oxygen reaction in an environment close to room temperature. Although the reaction is slow, due to the thickness of the coal seam, it will also consume a large amount of oxygen and produce a large amount of carbon monoxide. In addition, although many scholars have carried out research on different factors of low-oxygen gas emission, there are still shortcomings that the research factor is single[12−15] and the research conclusion is qualitative.[11,16] Therefore, there is a lack of systematic research on the low-oxygen phenomenon in the top coal caving working face of the ultrathick coal seam, and the research should focus on both the oxygen consumption mechanism of residual coal at low temperatures (even room temperature) and the emission law of low-oxygen gases under different influencing factors.

2. ENGINEERING BACKGROUND

Madaotou coal Mine is located in Zuoyun County, Shanxi Province, China, in the south of the Datong coal field. The mine industrial square is approximately 45 km east of Datong City and 15 km west of Zuoyun County. The geographic location is in the east longitude: 112°37′01″−112°51′03″ and north latitude: 39°46′48″−39°53′25″. The length of the coalfield is about 20.087 km from east to west and 12.575 km from north to south, with an authorized mining area of about 197.8132 km^2. The ventilation method of the mine is a hybrid, and the ventilation method is mechanical extraction. The 8105 top coal caving working face mainly mines the 5(3-5)# coal seam, with a burial depth of 300−460 m, an average inclination angle of 3°, a strike length of 2,288 m, a dip length of 220 m, a total thickness of 5.76−22.98 m, and an average

https://doi.org/10.1021/acsomega.4c02310
ACS Omega 2024, 9, 33679−33691

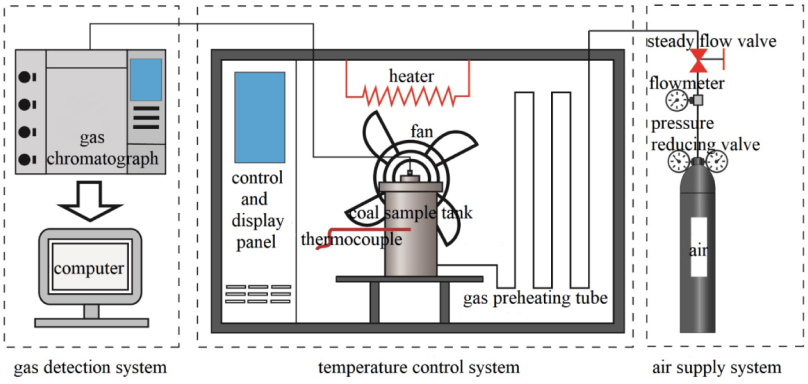

Figure 2. Programmed temperature-raising box and gas chromatography coupling equipment.

coal thickness of 17.8 m. The mechanical coal cutting height of the 8105 working face is 3.9 m, the top coal caving height is 13.9 m, and the thickness of the residual coal is about 1.78 m.

The mining and ventilation system diagram of the 8105 top coal caving working face is shown in Figure 1. During the production of the 8105 working face in three states, that is, coal cutting, top coal caving, and equipment maintenance, the oxygen concentrations monitored at different locations in the air return corner are shown in Table 1. The oxygen concentration monitoring points were arranged near the air return corner, 1.5 m away from the coal wall of the air return roadway, with heights of 2.5 m, 1.5 m and 0.8 m, respectively. As can be seen from Table 1, there was a serious low-oxygen area near the working face during the production process of the 8105 working face in the Madaotou coal mine, and the composition of gas emitted from the air return corner of different working processes was significantly different, which posed a great threat to the safe production of the working face.

3. RESEARCH METHODS

3.1. Low-Constant Temperature Oxygen Consumption Program Heating Experiments. The low-temperature oxygen consumption and gas production experiments of coal left in the mining area were carried out by using a programmed temperature-raising box and gas chromatography coupling equipment (as shown in Figure 2).[17,18] The experimental coal samples were taken from the freshly exposed coal wall of the 8105 top coal caving working face of the Madaotou mine, wrapped in plastic wrap, transported back to the laboratory, and crushed in a vacuum environment. The properties of the coal sample are shown in Table 2.

Table 2. Properties of the Coal Sample

proximate analysis (wt %)			ultimate analysis (wt %, daf)				
M_{ad}	A_{ad}	V_{ad}	C	H	O	N	S
6.54	9.73	27.36	78.45	4.02	1.02	1.45	15.16

The specific experimental steps were as follows: (1) Screen out fresh coal samples with a particle size of 6−10 mm. (2) Load 800 g of coal samples into the sample tank and check the air tightness of the system. (3) Pass dry air for 5 min before the start of the experiments to discharge the impurity gas in the coal sample tank and the gas adsorbed on the surface of the coal sample. (4) Calibrate the gas chromatograph. (5) Increase the temperature in the program heating box to 30 °C, 40 °C, 50 °C, 60 °C, 70 °C in turn. (6) Inject dry air with a flow rate of 22 mL/min into the program heating box after it reached the set temperature. The time after 2 min of air injection was taken as the start time of every experiment. (7) Maintain each set temperature for 120 min and use the gas chromatograph to test the mixed gas at the outlet of the coal sample tank every 15 min. (8) Repeat each experiment three times to ensure accuracy. (9) Analyze the experimental results and master the characteristics of oxygen consumption and gas production of residual coal at low temperatures.

3.2. Low-Constant Temperature Oxygen Consumption Infrared Spectroscopy Experiments. The experimental research on the evolution of micro functional groups during the low-temperature oxygen consumption process of the residual coal in goaf was conducted by using an in situ Fourier infrared spectrometer (as shown in Figure 3).[19−21]

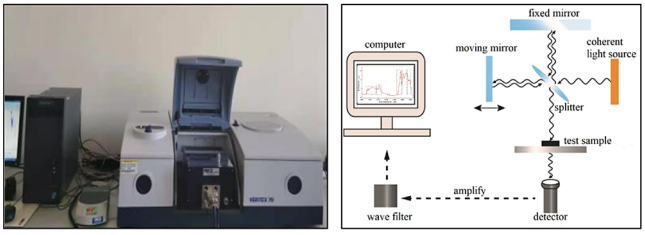

(a) equipment physical diagram (b) working principle diagram

Figure 3. In situ Fourier transform infrared spectrometer.

The specific experimental steps were as follows: (1) Screen out fresh coal samples with a particle size of 100−120 mesh. (2) Open the in situ Fourier transform infrared spectrometer analysis software, set the spectral scanning range to 4000−500 cm^{-1}, resolution to 2 cm^{-1}, scanning frequency to 64 times/s, and the unit of in situ spectral absorption intensity to Kubelka−Munk. (3) Bake KBr powder under an incandescent lamp for about 10 min, then load KBr into a sample cell, adjust the background light intensity to maximum, measure the background spectrum of the infrared spectrum, remove the sample cell, and pour out the KBr powder after the test is completed. (4) Put the prepared coal samples into the sample cell and measure the infrared absorption spectrum of the residual coal. (5) Increase the temperature in the reaction tank of the infrared spectrometer to 30 °C, 40 °C, 50 °C, 60 °C, and 70 °C in turn. (6) Inject dry air with a flow rate of 22 mL/min into the reaction tank after it reached the set temperature. The time after 2 min of air injection was taken as the start time of every experiment. (7) Maintain each set temperature for 120

https://doi.org/10.1021/acsomega.4c02310
ACS Omega 2024, 9, 33679−33691

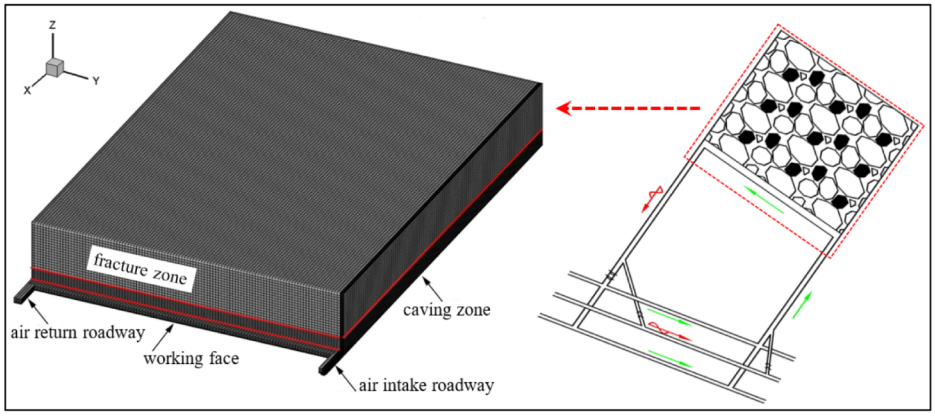

Figure 4. Schematic diagram of the geometric model.

min, and test the infrared absorption spectrum of the coal samples at the 30th, 60th, and 120th minutes of the same constant temperature. (8) Repeat each experiment three times to ensure accuracy. (9) Analysis the experimental results and master the evolution law of micro functional groups during the heating and oxidation processes of the residual coal in the goaf.

3.3. Numerical Simulation of the Influence of Different Factors on Low-Oxygen Gas Emission. At present, numerical calculation is the main tool for studying the gas migration process in large-scale mining areas.[22−27] Taking the 8105 working face of the Madaotou mine as the engineering background, Fluent^{3D} numerical calculation software was used to establish a numerical calculation model of the flow field in the working face of extra-thick spontaneous combustion coal seams. On this basis, the effects of nitrogen injection in the goaf and air intake in working face on the distribution of oxygen concentration in the mining area were studied. The numerical calculation physical model of the 8105 working face is shown in Figure 4. The ventilation method of the working face was U-type ventilation, the air intake was 2100 m^3/min, and the oxygen concentration in the air intake roadway was 0.21. The amount of residual coal in the goaf was determined by setting the oxygen consumption height, which was 1.78 m (Tables 3 and 4).

Table 3. Main Parameters of the Calculation Model

no.	model part	geometric dimensions
1	air intake roadway	length 20 m × width 5.1 m × height 3.9 m
2	air return roadway	length 20 m × width 5.1 m × height 3.9 m
3	working face	length 220 m × width 6.1 m × height 3.9 m
4	caving zone	length 300 m × width 220 m × height 20 m
5	fracture zone	length 300 m × width 220 m × height 80 m
6	nitrogen injection port	diameter 0.3 m

The coal and rock in the goaf are affected by the mining of the working face, forming a free accumulation porous medium area in the goaf. The movement of fluid in the goaf conforms to the theory of porous medium seepage. The motion of fluid in the goaf satisfies the mass and momentum conservation equations of a porous medium. The mass conservation equation in the porous medium is

$$\frac{\partial}{\partial t}(\gamma\rho_f) + \nabla(\gamma\rho_f\vec{v}) = S_m \tag{1}$$

Table 4. Boundary Conditions and Parameter Settings

category	boundary condition
inlet	velocity inlet
outlet	free outflow
workface, roadway, and goaf wall surfaces	non slip wall surface
porosity of porous medium in goaf	use UDF to import porosity function
O_2 consumption source term in goaf	set according to experimental and actual conditions
viscous and inertial resistance	use PROFILE macro definition
nitrogen injection port	velocity inlet

where γ is the porosity of porous media, m^{-3}; ρ_f is the mass density of the fluid, kg/m^3; ∇ is the Hamiltonian operator; $\vec{v}$ is the flow velocity of fluid in the porous medium, m/s; S_m is the gas mass source term, kg/m^3·s^{-1}.

The momentum conservation equation in the porous medium is

$$\frac{\partial}{\partial t}(\gamma\rho_f\vec{v}) + \nabla\cdot(\gamma\rho_f\vec{v}\vec{v}) = -\nabla p + \nabla\cdot(\bar{\bar{\tau}}) + \gamma\rho_f\vec{g} + S \tag{2}$$

where $\bar{\bar{\tau}}$ is the viscous stress tensor; p is gas pressure, Pa; S is the additional momentum loss source term during air flow migration in the porous medium. For the isotropic porous medium:[28]

$$S = -\left(\frac{\mu}{\alpha}v_i + C_2\frac{1}{2}\rho_f|v|v_i\right) \tag{3}$$

where μ is the dynamic viscosity coefficient of the fluid, kg/m·s^{-1}; α is the permeability; and C_2 is the coefficient of inertial resistance. According to Blake−Kozeny's derivation idea, the empirical formula for nonlinear flow condition is defined as[28]

$$\alpha = \frac{D_m{}^2 n^3}{150(1-n)^2} \tag{4}$$

$$C_2 = \frac{3.5}{D_m}\frac{(1-n)}{n^3} \tag{5}$$

where D_m is the average particle size of the falling rock in the goaf; and n is the porosity.

The oxygen diffusion equation is

$$\frac{\partial}{\partial t}(\rho Y_i) + \nabla\cdot(\rho\vec{v}Y_i) = -\nabla\cdot\vec{J}_i + R_i + S_i \tag{6}$$

https://doi.org/10.1021/acsomega.4c02310
ACS Omega 2024, 9, 33679−33691

where Y_i is the oxygen mass fraction; R_i is the net rate of oxygen chemical reaction generation, kg/m^3·s^{-1}; S_i is the oxygen generation rate, kg/m^3·s^{-1}; $\vec{J}_i$ is the diffusion flux of oxygen given by Fick's law, which in the turbulence model is expressed as

$$\vec{J}_i = -\left(\rho D_{i,\mathrm{m}} + \frac{\mu_t}{S_{c_t}}\right)\nabla Y_i - D_{\mathrm{T},i}\frac{\nabla T}{T} \tag{7}$$

where $D_{i,\mathrm{m}}$ is the mass diffusion coefficient of oxygen; $D_{\mathrm{T},i}$ is the thermal diffusion coefficient of component oxygen; S_{c_t} is the turbulent Schmidt number.

The distribution function of goaf porosity is as follows:

$$n = n_x n_y n_z = \begin{cases} 0.2\mathrm{e}^{-0.0223} + 0.1\cdot(\mathrm{e}^{-0.15y} + 0.1)\cdot 0.99^z & y < \dfrac{l}{2} \\ 0.2\mathrm{e}^{-0.0223} + 0.1\cdot(\mathrm{e}^{-0.15(220-y)} + 0.1)\cdot 0.99^z & y \geq \dfrac{l}{2} \end{cases} \tag{8}$$

where n_x, n_y, and n_z are the porosity along the dip length (y-axis), along the strike length (x-axis), and along the height of the goaf (z-axis) respectively; l is the total length of the working face. The distribution of porosity in the goaf is shown in Figure 5.

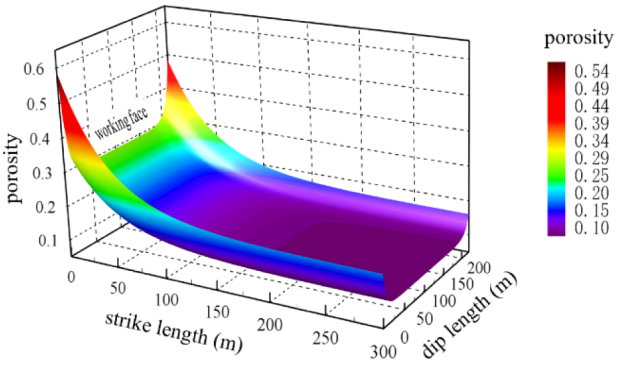

Figure 5. Distribution of the porosity in the goaf.

4. RESULTS AND DISCUSSION

4.1. Characteristics of Oxygen Consumption and Gas Production of Residual Coal at Low-Constant Temperature. Figure 6 shows the changes of the oxygen concentration in the low-constant temperature process. The O_2 consumption rate can be obtained by the change of O_2 concentration in the coal sample tank in Figure 2, and the calculation is given in eq 9.[17]

$$v_{\mathrm{O}_2}(T) = \frac{v_{\mathrm{g}} c^{\mathrm{i}}_{\mathrm{O}_2}}{(1-n)SL}\ln\frac{c^{\mathrm{i}}_{\mathrm{O}_2}}{c^{\mathrm{o}}_{\mathrm{O}_2}} \tag{9}$$

where $v_{\mathrm{O}_2}(T)$ is the O_2 consumption rate (mol/(cm^3·s)), v_{g} is the experimental supply air volume (mL/s), $c^{\mathrm{i}}_{\mathrm{O}_2}$ is the O_2 concentration at the inlet of coal sample tank (mol/cm^3), $c^{\mathrm{o}}_{\mathrm{O}_2}$ is the O_2 concentration at the outlet of coal sample tank (mol/cm^3), n is the porosity of the experimental coal sample, S is the cross-sectional area of the coal sample tank (cm^2), L is the length of the air inlet and outlet of the coal sample tank (cm).

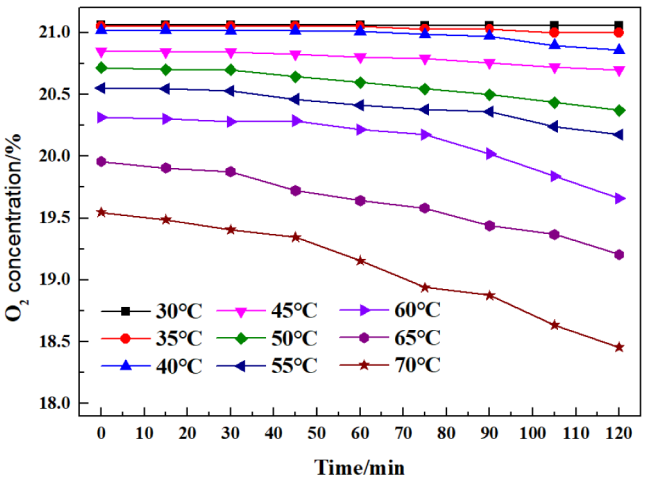

Figure 6. Variation law of the O_2 concentration.

Combined with the O_2 concentration in Figure 6 and eq 9, the rate of consumption of O_2 in the experiments can be obtained as shown in Figure 7.

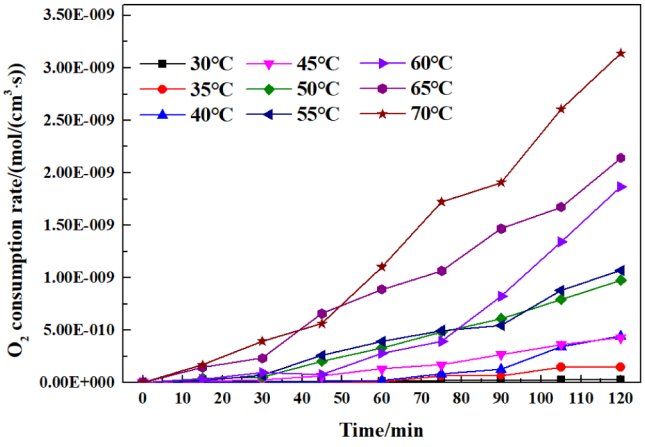

Figure 7. Variation law of the O_2 consumption rate.

As shown in Figures 6 and 7, during the low-constant temperature process, with the extension of residence time, the oxygen concentration in the mixed gas at the outlet of the coal sample tank decreased and the oxygen consumption rate increased. When the constant temperature was 30 and 35 °C, the oxygen concentration and oxygen consumption rate did not change significantly with the extension of residence time. When the constant temperature was 40 °C, there was a significant change in oxygen concentration and oxygen consumption rate after staying for 90 min. When the constant temperature was 45 °C, there was a significant change in oxygen concentration and oxygen consumption rate after staying for 75 min. When the constant temperature was 50 and 55 °C, the oxygen concentration and oxygen consumption rate began to show significant changes after staying for 60 min. When the constant temperature was 60 and 65 °C, there was a significant change in oxygen concentration and oxygen consumption rate after staying for 30 min. When the constant temperature was 70 °C, there were significant changes in oxygen concentration and oxygen consumption rate at the beginning of the constant temperature.

https://doi.org/10.1021/acsomega.4c02310
ACS Omega 2024, 9, 33679−33691

Figures 8 and 9 show the changes of CO generation and CO_2 generation in the low-constant temperature process,

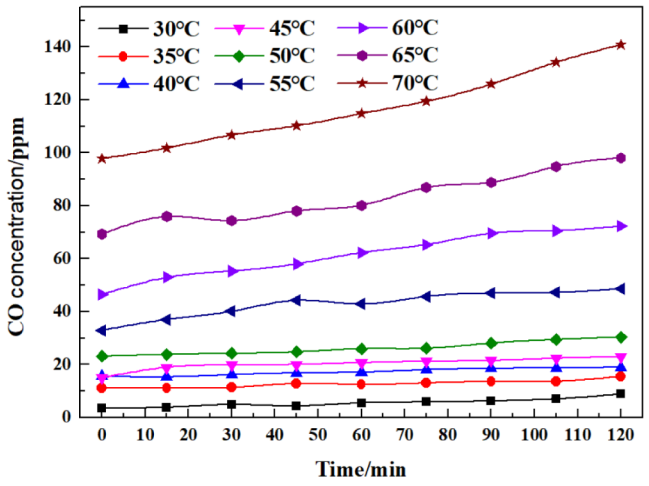

Figure 8. Variation law of the CO concentration.

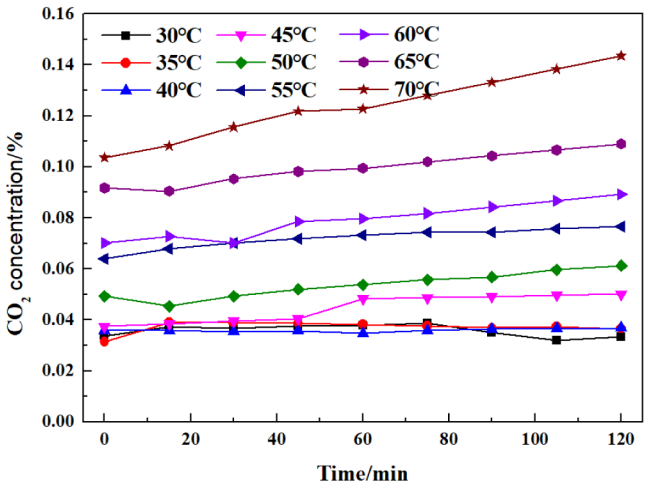

Figure 9. Variation law of the CO_2 concentration.

respectively. As shown in Figures 8 and 9, in the process of constant temperature, with the extension of time, the production of CO and CO_2 showed an overall rising trend. The above results can be scientifically explained by the active sites proposed by Li et al.[29−31] The original coal sample contains a small number of active sites, and at the same time, the low-temperature pyrolysis process of coal produces a large number of active sites, which can react with oxygen at low temperatures (even room temperature) to produce CO and CO_2. Under constant temperature conditions, with an extension of time, the number of active sites continues to increase, resulting in an increase in the generation of CO and CO_2. Wang et al.[32] also believed that the low-temperature oxidation process of coal involves multiple steps: adsorbing oxygen on the pore surface to form unstable coal oxygen intermediates, decomposing unstable solid coal oxygen intermediates to form gas and stable solid products, and thermal decomposition of stable composite products to form active sites. Active sites can scientifically reveal the results.

The difference in constant temperature affected the time of abrupt change in CO and CO_2 production. With the increase of constant temperature, the abrupt change in time of CO and CO_2 production was advanced. When the constant temperature was lower than 40 °C, the amount of CO and CO_2 generation did not change significantly with time, the amount of generation was also relatively low, and there was a rising trend after 100 min. When the constant temperature was higher than 40 °C, the constant temperature time had a great influence on the CO and CO_2 production, and the CO and CO_2 production increased linearly with the extension of the constant temperature time. The above results showed that when a large amount of residual coals remains in the oxidation zone (oxidation zone is defined as the goaf area with an oxygen concentration of 10−18%) for a long time, low-temperature oxidation consumes a large amount of oxygen and produces CO and CO_2 gases.

4.2. Evolution of Functional Groups during Oxygen Consumption and Gas Production of Residual Coal at Low-Constant Temperature. Figure 10 shows the infrared

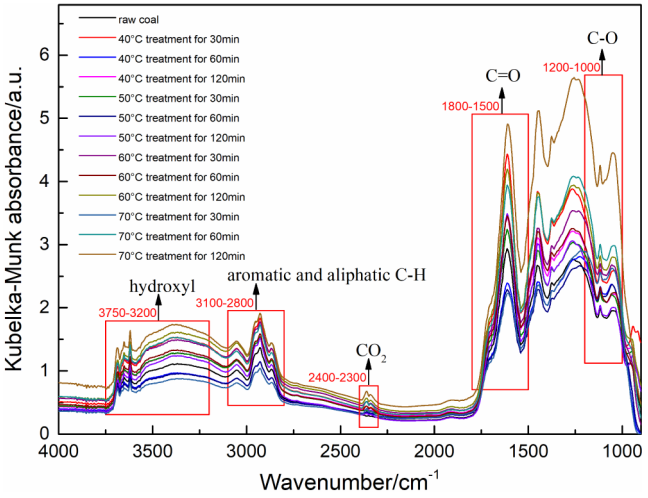

Figure 10. Infrared absorption spectrum of coal under different constant temperature conditions.

absorption spectrum of coal under different constant temperature conditions. As shown in Figure 10, the infrared spectrum of raw coal mainly contains five vibration ranges, namely, the hydroxyl stretching vibration range (3750−3200 cm^{-1}), aromatic and aliphatic C−H stretching vibration range (3000−2800 cm^{-1}), CO_2 stretching vibration range (2400−2300 cm^{-1}), C═O compound stretching vibration range (1800−1500 cm^{-1}), and alcohol, phenolic, and ether stretching vibration range (1200−1000 cm^{-1}). These micro functional groups affect the oxygen consumption characteristics of the original residual coal. The absorption peak positions of different functional groups were determined by calculating the second-order derivative of the original infrared spectral data, and the absorption peak areas of different functional groups were calculated by using the deconvolution peak fitting method.[33,34] Since there are many figures in the processing process, this paper takes raw coal as an example to demonstrate the second-order derivative and peak fitting process of the infrared spectrum (as shown in Figures 11 and 12, respectively). Research has shown that aliphatic C−H and aromatic C═O play a very important role in coal oxidation,[35] so the analysis of the microstructure of coal samples in this study is mainly based on these two types of functional groups.

https://doi.org/10.1021/acsomega.4c02310
ACS Omega 2024, 9, 33679−33691

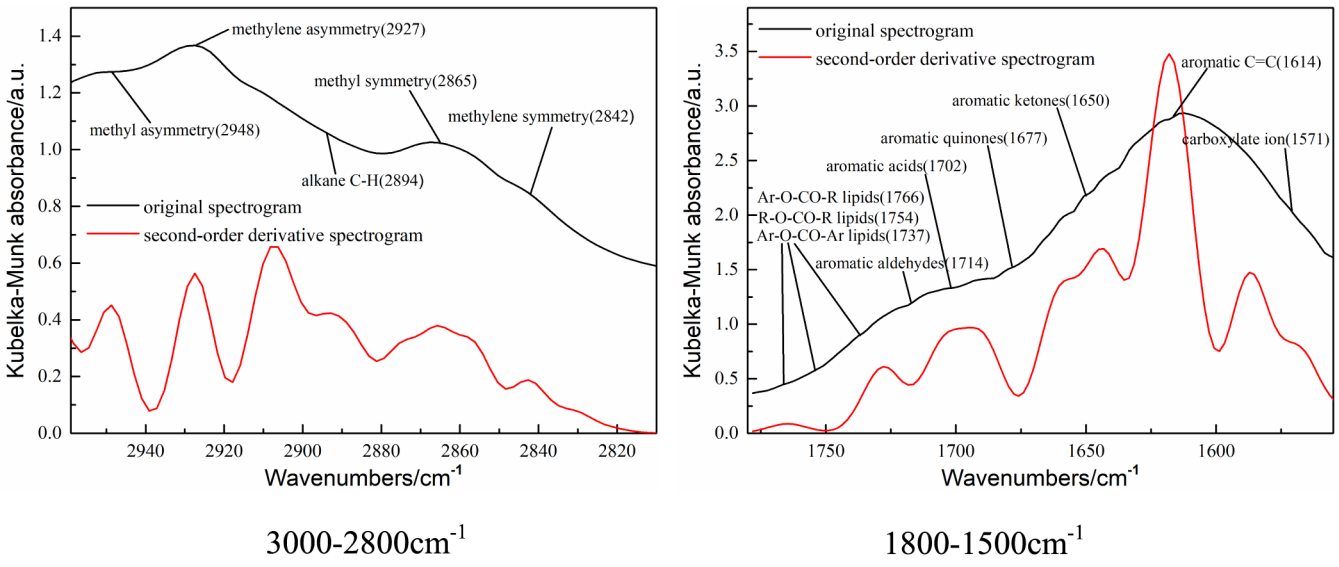

Figure 11. Second-order derivative analysis of the infrared absorption spectrum (raw coal).

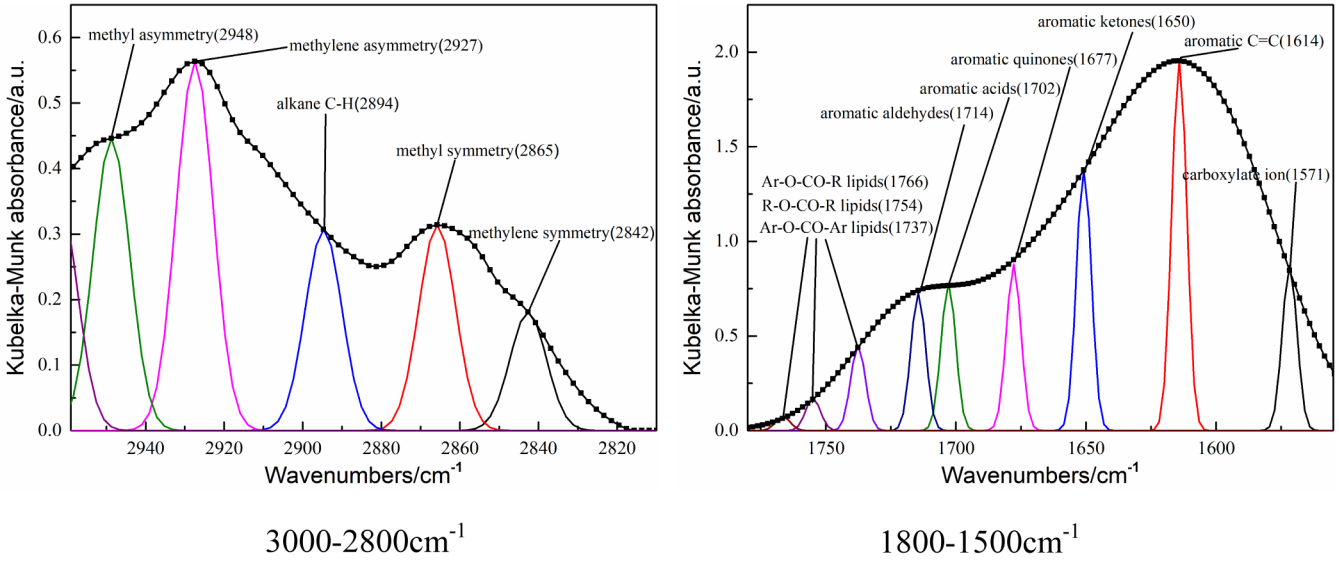

Figure 12. Peak fitting of the infrared absorption spectrum (raw coal).

The variation of the absorption vibration peak area of aliphatic C−H components in the process of low-constant temperature is shown in Figure 13. As shown in Figure 13, the peak area of aliphatic C−H components of coal samples generally decreased with the extension of the constant temperature time. The above results are basically consistent with previous studies.[36] When the thermostatic temperature was 40 °C, the duration of the constant temperature had little effect on the peak area of the aliphatic C−H component. When the thermostatic temperature was 50 °C, the effect began to be obvious. When the thermostatic temperature was 70 °C, the effect was the greatest. The above results show that when the temperature reached a certain value, the coal oxygen reaction became more intense and the coal oxidation degree became higher with the increase of the coal sample oxidation time. With the increase of constant temperature, the peak area of aliphatic C−H components decreased and the conversion rate of C−H components increased. This is because in the early stage of oxidation, the aliphatic C−H components were attacked by oxygen molecules and reacted with them.[35,36] When the temperature was low, the peak area of the C−H component decreased relatively gently and the conversion rate was relatively low. With the increase of temperature, the decreasing trend of the C−H component peak area decreased, indicating that the conversion rate increased. With the increase of temperature, the peak area changes of asymmetric methyl and methylene groups were more pronounced than those of alkane C−H and symmetric methyl and methylene groups, which indicated that during the heating process of coal samples, asymmetric methyl and methylene groups were more likely to combine with oxygen molecules to undergo oxidation reactions, while alkane C−H and symmetric methyl and methylene groups were more stable and less susceptible to oxidation reactions caused by oxygen molecules.[33] The conversion rate of methyl was lower than that of methylene, indicating that the oxidation of methylene was greater than that of methyl during the heating process.

https://doi.org/10.1021/acsomega.4c02310
ACS Omega 2024, 9, 33679−33691

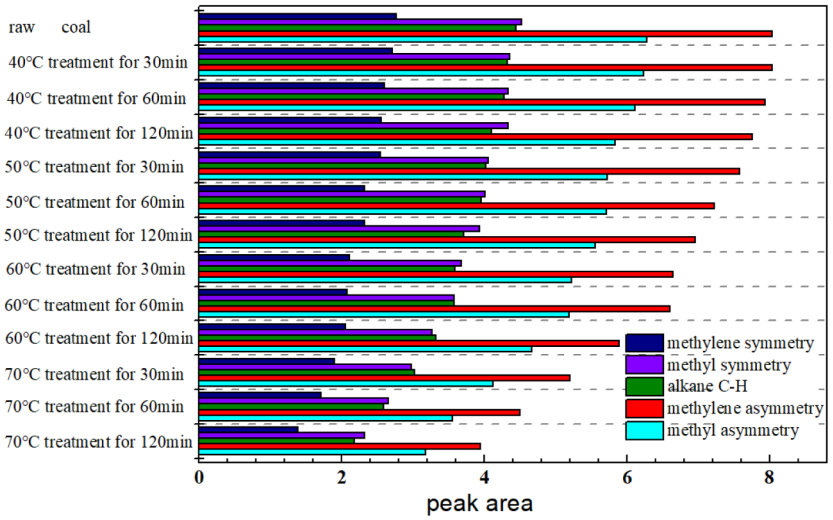

Figure 13. Variation of the absorption vibration peak area of aliphatic C−H components.

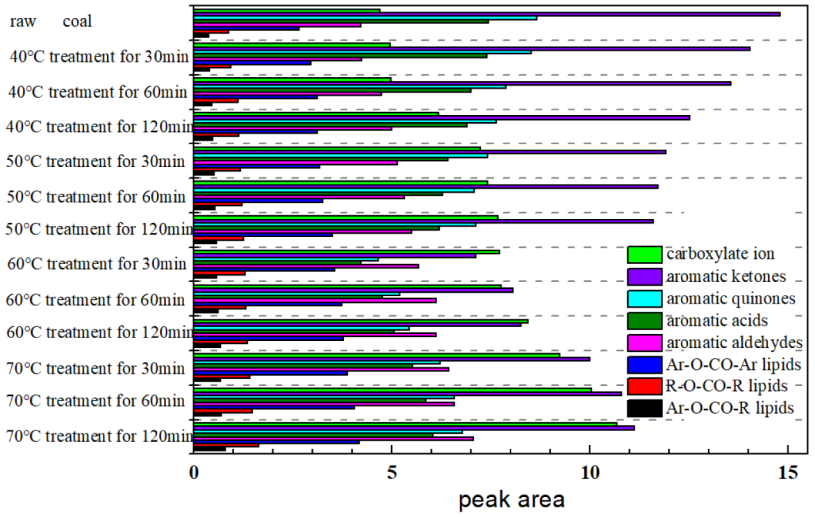

Figure 14. Variation of the absorption vibration peak area of aromatic C═O compounds.

The major absorption vibrational peaks in the 1800−1500 cm^{-1} absorption vibrational interval of coal samples were aromatic ketones, quinones, acids, aldehydes, lipids, aromatic C═C and carboxylate ions. Because the peak area of aromatic C═C did not change much during heating process, the main analysis was focused on the peak area changes of C═O compounds.[35,37] The variation of the absorption vibration peak area of C═O compounds during the constant temperature process is shown in Figure 14. As shown in Figure 14, except for aromatic acids, quinones, and ketones, which first increased and then decreased with the increase and extension of temperature and time, the other aromatic C═O compounds showed a continuous increasing trend with the increase and extension of temperature and time. The above phenomenon shows that at the low temperature stage of 40−70 °C, the aromatic C═O compounds in coal begin to transform continuously, which is basically consistent with the conclusion obtained by Li et al.[29−31] and Wu et al.[38] that the above functional groups may change at room temperature. The peak areas of aromatic acids, quinones, and ketones showed a significant decrease with the extension of the constant temperature at 40 °C, indicating that these three types of compounds could be easily decomposed at the early stage of coal oxidation. During the coal oxidation process, CO and CO_2 gases were mainly decomposed by aromatic ketones, aromatic quinones, and aromatic acid compounds. When the temperature was below 50 °C, the generation of these three types of compounds was less than the decomposition amount, and when the temperature was above 50 °C, it was greater than the decomposition amount. Zhang et al.[35] pointed out that active oxygenated species are the precursors for CO and CO_2 emissions during low-temperature coal oxidation and divided the active oxygenated species in the coal matrix into two categories: one is the original oxygen-containing functional groups in coal, and the other is the oxygen-containing complexes formed on the surface of coal by the attack of oxygen on active sites. The research results of this paper are consistent with the views of Zhang et al.

4.3. Influence of Nitrogen Injection Amount on Oxygen Concentration of Mining Space. At present, nitrogen injection in goaf is the most commonly used fire prevention and extinguishing technology in the top coal caving working face of ultrathick coal seams.[39−41] Nitrogen injection can significantly change the oxygen concentration in the gob

https://doi.org/10.1021/acsomega.4c02310
ACS Omega 2024, 9, 33679−33691

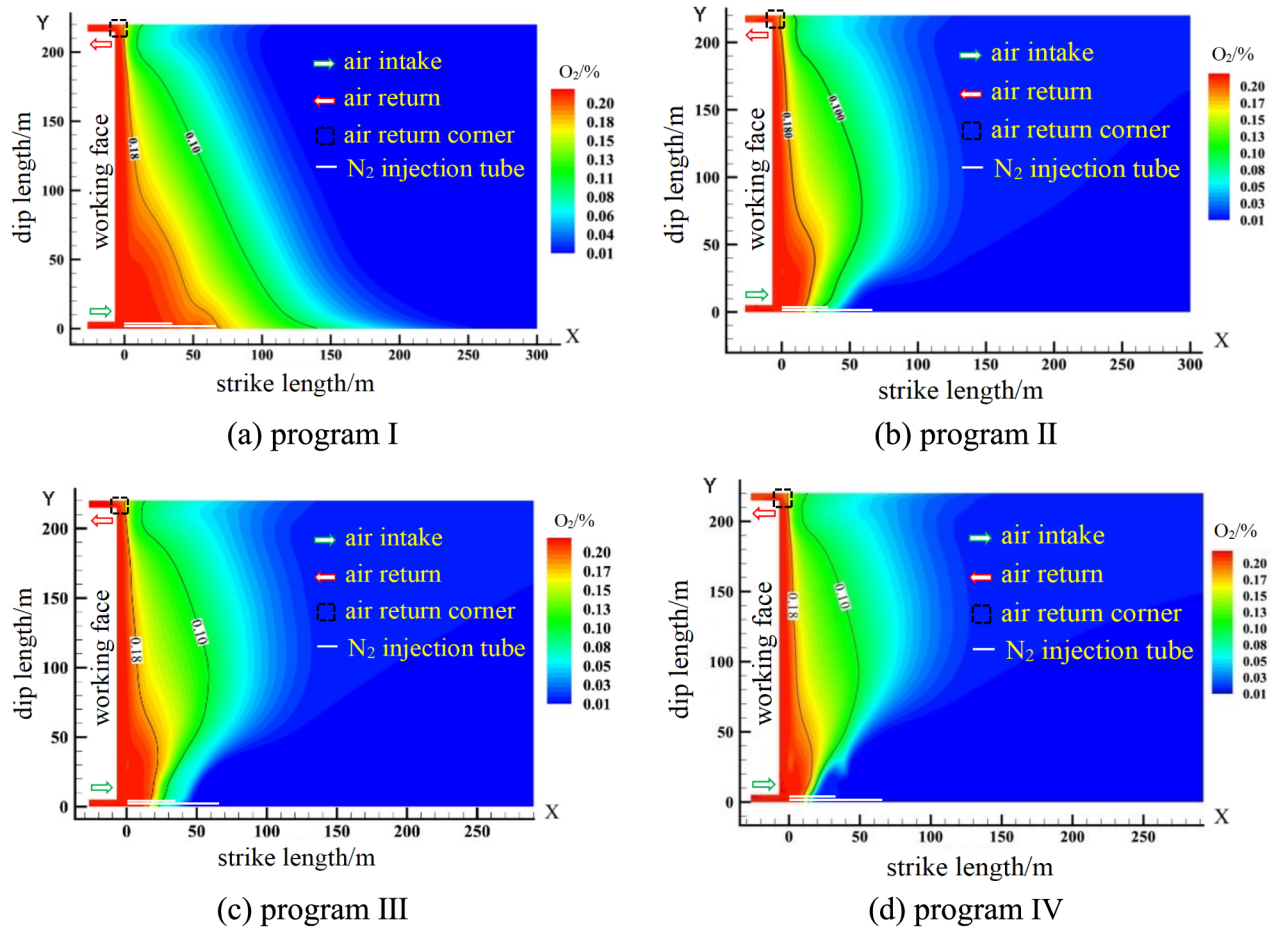

Figure 15. (a–d) O_2 concentration in the goaf under different N_2 injection programs (z = 2.4 m).

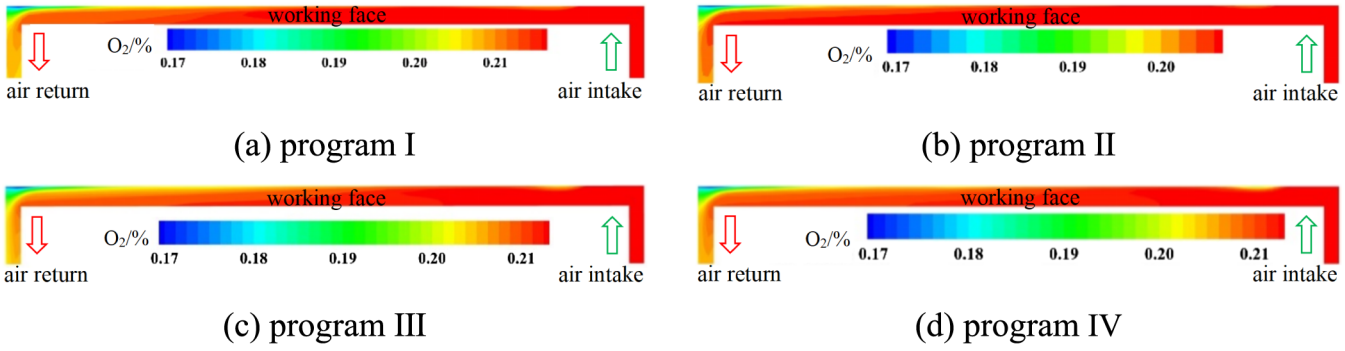

Figure 16. (a–d) O_2 concentration in the working face under different N_2 injection programs (z = 2.4 m).

and has a significant impact on the low-oxygen phenomenon in the working face. Therefore, it is necessary to conduct a systematic study on the influence of a single factor of nitrogen injection on the oxygen concentration of the mining space. Two nitrogen injection ports were set up in the model, and their locations were 35 m and 65 m in the goaf on the side of the air intake roadway. The diameter of the nitrogen injection tube was 0.3 m. Four comparison programs were set up in this study: (I) the nitrogen injection port speeds were 0 m/s and 0 m/s respectively; (II) the nitrogen injection port speeds were 1.57 m/s and 4.32m/s respectively, and the nitrogen injection volume was 1500 m^3/h; (III) the nitrogen injection rates were 2.07 and 4.79 m/s, respectively, and the nitrogen injection volume was 1745 m^3/h; (IV) the nitrogen injection port speeds were 2.36 m/s and 5.11 m/s, respectively, and the nitrogen injection volume was 1900 m^3/h.

Figure 15 shows the distribution of the oxygen concentration in the goaf under four different nitrogen injection programs. As shown in Figure 15, when the air intake was constant, the difference in the oxidation zone between nitrogen injection and non-nitrogen injection in the goaf was very obvious. With the increase of nitrogen injection, the width of oxidation zone narrowed and the range of oxidation zone moved forward from the deep part of the goaf. When there was no nitrogen injection in the goaf, the width of the oxidation zone narrowed from the side of the air intake roadway to the side of the air return roadway, and the width of the oxidation zone decreased from 70 m to 20 m, and the location of the

https://doi.org/10.1021/acsomega.4c02310
ACS Omega 2024, 9, 33679−33691

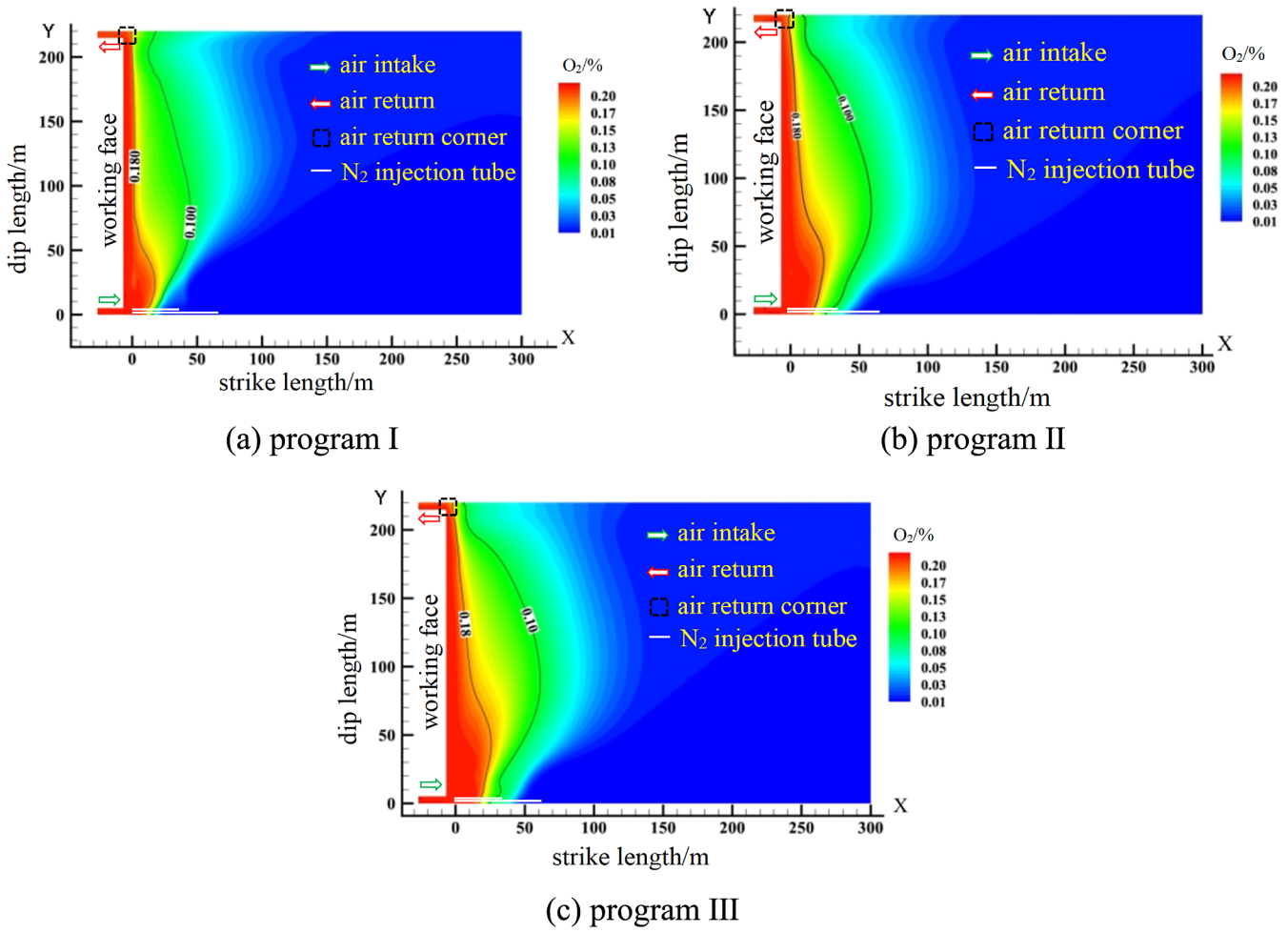

Figure 17. (a−c) O_2 concentration in the goaf under different ventilation programs (z = 2.4m).

oxidation zone moved forward from the deep part of the goaf. When nitrogen was injected into the goaf, the width of the oxidation zone decreased first, then increased, and then decreased from one side of the air intake roadway to the other side of the air return roadway. When the nitrogen injection volume was 1500 m^3/h, the width of the oxidation zone was 50 m. When the nitrogen injection volume was 1745 m^3/h, the width of the oxidation zone was 47 m. When the nitrogen injection volume was 1900 m^3/h, the width of the oxidation zone was 40 m. With the increase of nitrogen injection, the oxidation zone in the goaf moved forward to the working face. The above results indicated that with the increase of nitrogen injection, the inerting effect of residual coal spontaneous combustion in the goaf gradually enhanced.

Figure 16 shows the distribution of oxygen concentration in the working face under four different nitrogen injection programs. As shown in Figure 16, when the air intake volume was constant, the oxygen concentration in the air return roadway was generally lower than that in the air intake roadway. The oxygen concentration in the working face showed a continuously decreasing trend from the air intake corner to the air return corner. With the increase of nitrogen injection, the oxygen concentration in the air return corner gradually decreased and the low-oxygen area gradually expanded. With the increase of nitrogen injection, the distance between the low-oxygen area and the air intake corner of the working face was gradually shortened.

According to the research results, there is a connection between nitrogen injection and the low-oxygen phenomenon. Nitrogen injection can effectively compress the width of the oxidation zone in the goaf, and the compression effect increases with the increase of nitrogen injection amount; however, nitrogen injection will inevitably lead to a large amount of low-oxygen gas influx into the air return corner of the working face. In order to achieve the control of coal spontaneous combustion and low-oxygen composite disasters, the following balance method can be adopted in actual production: when $t = L_x/\nu > T$, there is a risk of spontaneous combustion in the goaf; when $t = L_x/\nu = T$, there is a risk of critical value of spontaneous combustion in the goaf; when $t = L_x/\nu < T$, there is no risk of spontaneous combustion in the goaf; where t is the time that the residual coal in the goaf stays within the oxidation zone, d. L_x is the width of the oxidation zone in the goaf under different nitrogen injection conditions, m; ν is the advancing speed of the working face, m/d; and T is the shortest spontaneous combustion time of the coal seam, d. In the actual production process, ν and T remain constant, and L_x keeps shrinking with the increase in nitrogen injection. When $t = L_x/\nu = T$, that is, $L_x = \nu \cdot T$ is the maximum allowed width of the oxidation zone, and the corresponding nitrogen injection amount is the critical value that takes into balance between spontaneous combustion and low-oxygen prevention.

4.4. Influence of Air Intake Volume on Oxygen Concentration of Mining Space. The air intake of the

https://doi.org/10.1021/acsomega.4c02310
ACS Omega 2024, 9, 33679−33691

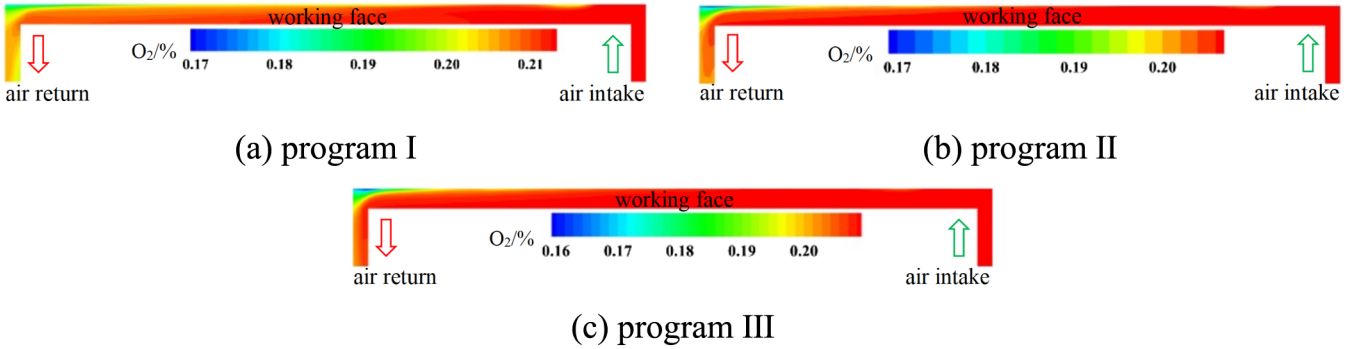

Figure 18. (a–c) O_2 concentration in the working face under different ventilation programs (z = 2.4 m).

working face provides the driving force for gas migration in the mining space and has a significant influence on the emission of low-oxygen gases in the top coal caving working face of ultrathick coal seams.[42,43] Therefore, it is necessary to conduct a systematic study on the influence of a single factor of air intake volume on the oxygen concentration of the mining space. In this study, the parameters of nitrogen injection remain unchanged. Two nitrogen injection ports were located 35 and 65 m away from the goaf in the side of the air intake roadway. The diameter of the nitrogen injection pipe was 0.3 m. The nitrogen injection port speeds were 1.57 and 4.32 m/s, respectively. The nitrogen injection volume was 1500 m^3/h. Three comparison programs were set up in this study: (I) the air intake velocity was 1.59 m/s, and volume was 1900 m^3/min; (II) the air intake velocity was 1.76 m/s, and the volume was 2100 m^3/min; (III) the air intake velocity was 1.93 m/s, and the volume was 2300 m^3/min.

Figure 17 shows the distribution of the oxygen concentration in the goaf under three different air intake volume programs. As shown in Figure 17, when the air intake volume was 1900 m^3/min, 2100 m^3/min, and 2300 m^3/min, the maximum width of the oxidation zone was 45 m, 47 m, and 50 m, respectively. With the increase of air intake volume, the width of the oxidation zone in the goaf increased, and the contour line with an oxygen concentration of 0.1 moved toward the deep part of the goaf.

Figure 18 shows the distribution of the oxygen concentration in the working face under the three different air intake volume programs. As shown in Figure 18, with the increase in air intake volume, the oxygen concentration in most areas of the air return roadway increased. When the air intake volume was 2300 m^3/min, the oxygen concentration in the air return roadway was basically the same as that in the air intake roadway. However, with the increase of air intake volume, the degree of low oxygen in the air return corner gradually intensified. When the air intake volume was 1900 m^3/min and 2100 m^3/min, the decrease of oxygen concentration occurred at about 30 m from the air intake corner, which was because the smaller air intake volume could not effectively dilute the high concentration of nitrogen leaking into the working face from the goaf.

According to the research results, there is also a connection between ventilation and the low-oxygen phenomenon. Increasing the air volume can dilute the gas in the roadway but increase the emission of low-oxygen gases in the goaf. In actual production, the optimal ventilation volume should be determined through reasonable experiments in the early stage, according to the actual situation of the mine.

5. CONCLUSIONS

Using a temperature-raising box and gas chromatography coupling equipment, the characteristics and mechanism of low temperature oxygen consumption of residual coal in goaf were obtained. The raw residual coal in goaf consumed a large amount of oxygen near 40 °C, accompanied by the generation of CO and CO_2. When the temperature was constant, the rates of oxygen consumption and gas production of residual coal increased gradually with time. In the low-temperature oxygen consumption process of residual coal, asymmetric methyl and methylene were more likely to undergo an oxidation reaction and generate carbonyl-containing compounds. The CO and CO_2 gases in the oxidation process of residual coal were mainly generated by the decomposition of aromatic ketones, aromatic quinones, and aromatic acids, and the generation of these three types of compounds was less than the amount of decomposition when the temperature was lower than 50 °C, and the generation was more than the amount of decomposition when the temperature was higher than 50 °C.

Using Fluent^{3D} numerical calculation software, we obtained the influence of different factors on the emission of low-oxygen gases in goaf. With the increase of nitrogen injection, the overall width of oxidation zone narrowed and the range of oxidation zone moved forward from the depth of the goaf. The oxygen concentration in the air return corner decreased gradually, and the low-oxygen area in the air return corner expanded gradually. The distance between the low-oxygen area of the working face and the air intake corner was gradually shortened. With the increase of air intake volume, the width of oxidation zone in the goaf increased and moved to the depth of the goaf. The oxygen concentration in the roadway increased, but the low-oxygen degree in the air return corner increased. In order to reduce the risk of low-oxygen in the top coal caving working face of ultrathick coal seams, the nitrogen injection amount should be reasonably set and the optimal air intake volume should be determined.

The causes of low oxygen in the top coal caving working face of ultrathick coal seams are mainly divided into two categories: the existence of low-oxygen concentration gas and the emission power of low-oxygen concentration gas. Low-oxygen gas can be provided by the large-scale, long-term, low-temperature oxygen consumption of residual coal, and nitrogen injection further aggravates the low-oxygen phenomenon. Ventilation makes low-oxygen gases in the goaf to continuously gush out to the working face, which has an important influence on the distribution of the low-oxygen area.

https://doi.org/10.1021/acsomega.4c02310
ACS Omega 2024, 9, 33679−33691

AUTHOR INFORMATION

Corresponding Authors

Jia Liu − *College of Safety and Emergency Management Engineering, Taiyuan University of Technology, Taiyuan 030024, China;* orcid.org/0000-0002-8757-3455; Email: 15135150829@163.com

Peng Liu − *School of Resources and Safety Engineering, Chongqing University, Chongqing 400000, China;* Email: liupengfirstone@163.com

Authors

Xu Zheng − *College of Safety and Emergency Management Engineering, Taiyuan University of Technology, Taiyuan 030024, China;* orcid.org/0009-0004-5056-8267

Xiaoping Liu − *Lu'an Chemical Group Co., Ltd., Changzhi 046204, China*

Ping Luo − *Shanxi Cooking Coal Group Co., Ltd., Taiyuan 030024, China*

Guangzu Hao − *College of Safety and Emergency Management Engineering, Taiyuan University of Technology, Taiyuan 030024, China*

Hongwei Liu − *College of Safety and Emergency Management Engineering, Taiyuan University of Technology, Taiyuan 030024, China; Lu'an Chemical Group Co., Ltd., Changzhi 046204, China;* orcid.org/0000-0003-2943-5553

Tingting Cai − *College of Safety and Emergency Management Engineering, Taiyuan University of Technology, Taiyuan 030024, China*

Complete contact information is available at: https://pubs.acs.org/10.1021/acsomega.4c02310

Notes

The authors declare no competing financial interest.

ACKNOWLEDGMENTS

This work was supported by the National Natural Science Foundation of China (No. 52304246); the Research Project supported by Shanxi Scholarship Council of China (No. 2023-057); the Basic Research Program (Free Exploration) Project of Shanxi Province (Nos. 20210302124222, 202303021222021, and 202303021221009); the Higher Education Science and Technology Innovation Project of Shanxi Province (No. 2021L050); the School Fund Project of Taiyuan University of Technology (No. 2022QN136).

REFERENCES

(1) Wu, B.; Wang, J. X.; Zhong, M. Y.; Xu, C. C.; Qu, B. L. Multidimensional analysis of coal mine safety accidents in China-70 years review. *Min. Metall. Explor.* **2023**, *40* (1), 253−262.

(2) Onifade, M. Countermeasures against coal spontaneous combustion: a review. *Int. J. Coal Prep. Util.* **2022**, *42* (10), 2953−2975.

(3) Zheng, X.; Ge, S. C.; Liu, H. W.; Liu, J.; Yan, J. J. Research on the characteristics and control technology of gas disasters in the gob of the nonpillar working face based on the DEM-CFD coupled model. *ACS Omega* **2024**, *9* (3), 3758−3771.

(4) Liu, J.; Qin, Y. P.; Zhou, T. B.; Gao, Y. Dual-porosity coupled borehole gas flow model: A new method for inversion of coal seam permeability. *Nat. Resour. Res.* **2020**, *29* (6), 3957−3971.

(5) Liu, J.; Qin, Y. P.; Zhang, S.; He, C. Numerical solution for borehole methane flow in coal seam based on a new dual-porosity model. *J. Nat. Gas Sci. Eng.* **2019**, *68*, 102916.

(6) Ren, T.; Qiao, M.; Roberts, J.; Hines, J.; Chow, Y. W.; Zong, W.; Sugden, A.; Shepherd, M.; Farrelly, M.; Kennedy, G.; et al. Development and evaluation of an immersive VR-CFD-Based tool for dust exposure mitigation in underground tunnelling operations. *Tunn. Undergr. Space Technol.* **2024**, *143*, 143.

(7) He, M. C.; Wang, Q. Rock dynamics in deep mining. *Int. J. Min. Sci. Technol.* **2023**, *33* (9), 1065−1082.

(8) Wu, M. L.; Ye, Y. C.; Hu, N. Y.; Wang, Q. H.; Tan, W. K. Visualization analysis and progress of mine water inrush disaster-related research. *Mine Water Environ.* **2022**, *41* (3), 599−613.

(9) Liu, H.; Wang, F. Thermal characteristics and kinetic analysis of coal-oxygen reaction under the condition of inert gas. *Int. J. Coal Prep. Util.* **2022**, *42*, 846−862.

(10) Qiao, M.; Ren, T.; Roberts, J.; Liu, H.; Yang, X.; Tan, L.; Wu, J. Improved computational fluid dynamics modelling of coal spontaneous combustioncontrol and gas management. *Fuel* **2022**, *324*, 124456.

(11) Wang, K.; Ai, Z.; Zhao, W.; Fu, Q.; Zhou, A. A hybrid model for predicting low oxygen in the return air corner of shallow coal seams using random forests and genetic algorithm. *Appl. Sci.-Basel.* **2023**, *13*, 2538.

(12) Gulawani, S. S.; Dahikar, S. K.; Joshi, J. B.; Shah, M. S.; RamaPrasad, C. S.; Shukla, D. S. CFD simulation of flow pattern and plume dimensions in submerged condensation and reactive gas jets into a liquid bath. *Chem. Eng. Sci.* **2008**, *63* (9), 2420−2435.

(13) Wasilewski, S. Influence of barometric pressure changes on ventilation conditions in deep mines. *Arch. Min. Sci.* **2014**, *59* (3), 621−639.

(14) Lolon, S. A.; Brune, J. F.; Bogin, G. E., Jr; Juganda, A. Study of methane outgassing and mitigation in longwall coal mines. *Min. Metall. Explor.* **2020**, *37* (5), 1437−1449.

(15) Lolon, S. A.; Brune, J. F.; Bogin, G. E., Jr; Grubb, J. W.; Saki, S. A.; Juganda, A. Computational fluid dynamics simulation on the longwall gob breathing. *Int. J. Min. Sci. Technol.* **2017**, *27* (2), 185−189.

(16) Chen, H.; Shao, H.; Jiang, S.; Huang, C.; Liu, G.; Li, S. Study on the cause of hypoxia in the corner of return air of shallow buried flammable coal seam group mining face and the coordinated prevention and control of coal spontaneous combustion. *Appl. Sci.-Basel.* **2023**, *13*, 7396.

(17) Liu, H.; Wang, F.; Ren, T.; Qiao, M.; Yan, J. Influence of methane on the prediction index gases of coal spontaneous combustion: A case study in Xishan coalfield, China. *Fuel* **2021**, *289*, 119852.

(18) Liu, H.; Wang, F.; Ren, T. Research on the Characteristics of the Coal−Oxygen Reaction in a Lean-Oxygen Environment Caused by Methane. *Energy Fuels* **2019**, *33* (9), 9215−9223.

(19) Gao, F.; Jia, Z.; Bai, Q. H.; Dong, J. J. Characteristics and mechanism of glutathione in inhibiting coal spontaneous combustion. *Fuel* **2023**, *352*, 129006.

(20) Liu, H.; Li, Z. H.; Yang, Y. L.; Miao, G. D.; Han, Y. Z. Effects of oxidation on physical and chemical structure of a low rank sub-bituminous coal during the spontaneous combustion latency. *Energy* **2023**, *272*, 127122.

(21) Dong, H.; Hu, X. M.; Yu, A. Q.; Wang, W.; Zhao, Q. K.; Wei, H. B.; Yang, Z. Y.; Wang, X. W.; Luo, C. Y. Study on the mechanism of an enteromorpha-based compound inhibitor for inhibiting the spontaneous combustion of coal using in situ infrared spectroscopy and thermal analysis kinetics. *J. Environ. Chem. Eng.* **2023**, *11* (2), 109577.

(22) Zhang, J.; Liang, Y. T.; Ren, T.; Wang, Z. W.; Wang, G. D. Transient CFD modelling of low-temperature spontaneous heating behaviour in multiple coal stockpiles with wind forced convection. *Fuel Process. Technol.* **2016**, *149*, 55−74.

(23) Wang, Z. W.; Ren, T.; Cheng, Y. P. Numerical investigations of methane flow characteristics on a longwall face Part I: Methane emission and base model results. *J. Nat. Gas Sci. Eng.* **2017**, *43*, 242−253.

(24) Ren, T.; Wang, Z. W.; Liang, Y. T.; Zhang, J. Numerical investigation of CO_2 fringe behaviour on a longwall face and its control. *Int. J. Coal Geol.* **2018**, *186*, 80−96.

(25) Qiao, M.; Ren, T.; Roberts, J.; Yang, X. H.; Li, Z. B.; Wu, J. M. New insight into proactive goaf inertisation for spontaneous combustion management and control. *Process Saf. Environ. Prot.* **2022**, *161*, 739−757.
(26) Qiao, M.; Ren, T.; Roberts, J.; Li, Z. B.; Wu, J. M. Ventilation arrangement evaluation and proactive goaf inertisation for spontaneous combustion and gas explosion management during longwall panel sealing-off process. *Environ. Sci. Pollut. Res.* **2023**, *30*, 115199−115227.
(27) Qiao, M.; Ren, T.; Roberts, J.; Liu, H. W.; Yang, X. H.; Tan, L. H.; Wu, J. M. Improved computational fluid dynamics modelling of coal spontaneous combustion control and gas management. *Fuel* **2022**, *324*, 124456.
(28) Tan, B.; Shen, J.; Zuo, D.; Guo, X. Numerical analysis of oxidation zone variation in goaf. *Procedia Eng.* **2011**, *26*, 659−664.
(29) Li, J. H.; Li, Z. H.; Yang, Y. L.; Duan, Y. J.; Xu, J.; Gao, R. T. Examination of CO, CO_2 and active sites formation during isothermal pyrolysis of coal at low temperatures. *Energy* **2019**, *185*, 28−38.
(30) Li, J. H.; Li, Z. H.; Yang, Y. L.; Wang, C. J. Study on oxidation and gas release of active sites after low-temperature pyrolysis of coal. *Fuel* **2018**, *233*, 237−246.
(31) Li, J. H.; Lu, W.; Li, J. L.; Yang, Y. L.; Li, Z. H. Mutual conversion of active sites and oxygen-containing functional groups during low-temperature oxidation of coal. *Energy* **2023**, *272*, 127151.
(32) Wang, H.; Dlugogorski, B. Z.; Kennedy, E. M. Kinetic modeling of low-temperature oxidation of coal. *Combust. Flame* **2002**, *131* (4), 452−464.
(33) Zhang, Y. L.; Wang, J. F.; Xue, S.; Wu, J. M.; Chang, L. P.; Li, Z. F. Kinetic study on changes in methyl and methylene groups during low-temperature oxidation of coal via in-situ FTIR. *Int. J. Coal Geol.* **2016**, *154*, 155−164.
(34) Zhou, C. S.; Zhang, Y. L.; Wang, J.; Wang, J. F.; Wu, Y. G.; Wu, J. M. Study on Intrinsic Relationship between Coal Mass Change and Heat Evolution during Different Stages of Coal Spontaneous Combustion. *Combust. Sci. Technol.* **2021**, *193* (14), 2445−2463.
(35) Zhang, Y. L.; Wang, J. F.; Wu, J. M.; Xue, S.; Li, Z. F.; Chang, L. P. Modes and kinetics of CO_2 and CO production from low-temperature oxidation of coal. *Int. J. Coal Geol.* **2015**, *140*, 1−8.
(36) Deming, W.; Zhong, X.; Junjie, G.; Xuyao, Q.I. Changes in active functional groups during low-temperature oxidation of coal. *Min. Sci. Technol.* **2010**, *20* (1), 35−40.
(37) Lopez, D.; Sanada, Y.; Mondragon, F. J. F. Effect of low-temperature oxidation of coal on hydrogen-transfer capability. *Fuel* **1998**, *77* (14), 1623−1628.
(38) Wu, Y. G.; Zhang, Y. L.; Zhou, C. S.; Wang, J. F.; Wu, J. M.; Ren, T. Study of CO sources and early-warning concentration of spontaneous combustion at air return corner in fully mechanized mining faces. *Combust. Sci. Technol.* **2021**, *193* (9), 1587−1604.
(39) Ding, C.; Li, Z. X.; Wang, J. R.; Lu, B.; Gao, D. M. Effects of inert gas CO_2/N_2 injection on coal low- temperature oxidation characteristic: Experiments and simulations. *Arabian J. Chem.* **2023**, *16* (2), 104510.
(40) Li, Z.; Wang, L.; Xie, X. C.; Pan, R. K.; Wang, X. H. N_2 inhibition characteristics of coal spontaneous combustion in goaf: experimental study and numerical analysis. *Combust. Sci. Technol.*, 2023.
(41) Liu, H.; Wang, F. Research on N_2-inhibitor-water mist fire prevention and extinguishing technology and equipment in coal mine goaf. *PLoS One* **2019**, *14* (9), No. e0222003.
(42) Rao, S.; Mishra, D. P.; Mishra, A. Methane migration and explosive fringe localisation in retreating longwall panel under varied ventilation scenarios: a numerical simulation approach. *Environ. Sci. Pollut. Res.* **2023**, *30* (25), 66705−66729.
(43) Tutak, M.; Brodny, J. Analysis of the impact of auxiliary ventilation equipment on the distribution and concentration of methane in the tailgate. *Energies* **2018**, *11* (11), 3076.

https://doi.org/10.1021/acsomega.4c02310
ACS Omega 2024, 9, 33679−33691